

Opportunities from Remote Sensing for Supporting Water Resources Management in Village/Valley Scale Catchments in the Upper Indus Basin

Nathan Forsythe · Hayley J. Fowler · Chris G. Kilsby · David R. Archer

Received: 1 November 2010 / Accepted: 7 October 2011 /
Published online: 3 November 2011
© Springer Science+Business Media B.V. 2011

Abstract Now and in the future, the flows of the Upper Indus Basin (UIB) are and will be depended upon by hundreds of millions of people for their food security and economic livelihoods. Communities in the headwater reaches of the UIB—which contribute the bulk of runoff for the basin—are equally deserving of improved living conditions, but often lag behind downstream communities in benefitting from infrastructure. Harsh and highly variable climatic conditions pose specific challenges for local agricultural activities in the headwater reaches. Improved scientific understanding of tributary basin scale hydrology should support local development work as well as improvements to large scale infrastructure and water resource management. This study focuses on the challenge of providing meaningful quantitative information at the village/valley scale in the upper reaches of the UIB. The typology of the UIB hydrological regimes—as observed in large gauged basins—are examined, with special emphasis on annual cycles and interannual variability. Variations in river flows (as relative anomalies of discharge rates or runoff) are compared to observations of climate parameters (2 m air temperature, precipitation) from both local (point-based) observations and analogous parameters from remote sensing data products from the MODIS instrument. Although the temporal overlap is limited between river gauging data available to this study and the MODIS observational record, numerical analysis of relationships between relative anomalies in the spatial data and river gauging observations demonstrate promising potential of the former to serve as quantitative indicators of runoff anomalies. In order to translate these relationships to the scale of ungauged village/valley catchments, the available remotely sensed spatial data—snow covered area (SCA), land surface temperature derived (LST)—are assessed as analogues for meteorological point observations. The correlations between local (point-based) observations and remotely-sensed spatial data products are tested across a wide range of spatial aggregations. These spatial units range from the primary contributing area (nearly

N. Forsythe (✉) · H. J. Fowler · C. G. Kilsby
Water Resource Systems Research Laboratory, School of Civil Engineering & Geosciences, Newcastle University, Newcastle upon Tyne, UK
e-mail: nathan.forsythe@newcastle.ac.uk

D. R. Archer
JBA Consulting, South Barn, Broughton Hall, Skipton, North Yorks, England BD23 3AE, UK

200,000 km²) of the UIB at its downstream gauging station Besham to a small valley serving a minor settlement (10 km²). The shape and timing of annual cycles in SCA and LST are consistent across the range of spatial scales although the magnitudes of both intra-annual and interannual variability differ with both spatial scale and hydrological regime. The interannual variability exhibited by these spatial data products is then considered in terms of its potential implications for the smaller hydrological units. Opportunities for improvement and extension of this methodology are also discussed.

Keywords Indus · Remote sensing · Snow · Temperature · MODIS

1 Introduction

1.1 Context of the Upper Indus Basin and its Headwater Reaches

The Upper Indus Basin (UIB) covers a vast expanse of high-mountain Asia. Its water resources are of the utmost importance to the wellbeing of Pakistan. It underpins local incomes and nutrition through irrigated agriculture and electricity supplies through hydropower. To partially summarise the comprehensive overview of water resources management issues in the Indus Basin by Archer et al. (2010) :

- Agricultural output from irrigated land provides 85% of cereal grain (wheat, rice) harvests as well as all sugar production.
- The agricultural sector accounts for 45% of the total labour force in Pakistan, and exports are dominated by goods derived from agricultural production—textiles (67%) and food items (11%).
- The hydropower generation of the Tarbela dam alone supplies nearly 20% of national electricity demand.

Thus without the contribution of the Indus, Pakistan's existing problems of food security & electrical load-shedding would be much greater. Pakistan's further socio-economic development thus depends largely on optimisation of its precious water resources.

Although the rugged headwaters of the UIB generate nearly all of the water for Pakistan's massive hydropower and irrigated agriculture schemes, local development has lagged behind much of the rest of the country. Analysis of local scale hydrological variability will focus on answering key questions posed by the development initiatives of two locally active international NGOs: the Aga Khan Rural Support Programme (AKRSP) & World Wildlife Fund (WWF)-Pakistan. AKRSP focuses primarily on improving community welfare through development of small-scale infrastructure—irrigation and mini-hydropower—to support local agriculture, industry and commerce. WWF focuses on sustainable natural resource management and ecosystem protection. Both NGOs place great emphasis on training and capacity building for community members. The analyses presented here aim to support the design of small-scale infrastructure and operational water resources management by assessment of the variability and interlinkages found in data available from both local observations and remote sensing. Techniques for extrapolating the hydrological implications of local weather observations for large basins have previously been established. This study will modify these techniques for application to the individual selected village/valley catchments by using remote sensing-derived data products as analogues for point measurements.

1.2 Description of Practical Outputs Needed from Hydrological Studies

Present water resources management challenges in the headwater reaches of the UIB, like those further downstream, are primarily due to the considerable interannual variability in flows and in the timing of the rising limb of the meltwater-driven hydrograph. In the future this variability will continue to complicate resource management, but water stresses in Pakistan will above all be driven by high demographic growth [Archer et al. 2010]. Unlike downstream areas where absolute per capita water scarcity will be the primary challenge in the future, for upstream reaches potential national pressure to limit abstractions—thus maintaining runoff transmission to the lower basin—combined with very limited arable land area to meet food security needs may become the driving concerns.

Given the current composition of local economic activities, the primary water resources management imperatives in the headwater reaches are to maximise crop yields from irrigated agriculture and electricity production from small and medium-scale hydropower. Local electricity demands are greatest during the (cold, dark) winter season when flows are low and exhibit relatively low variability. Electrical grid transmission infrastructure necessary to export electricity to other regions at present is, and for the foreseeable future will be, lacking. The primary nexus of opportunity and need for improvement in water resources management is thus to support irrigated agricultural activities concentrated in the warm, hydrologically variable, summer season.

The two principal potential applications of hydrological insight in the UIB for support of local development initiatives are : i) improvement of present operational water resources management (water allocation in irrigation) via skilled seasonal forecasts; & ii) improved infrastructure design and long term planning via confident characterisation of future water availability, including its variability. Specific examples of this infrastructure include irrigation systems covering tens or hundreds of hectares and mini-hydropower systems with rated capacities in the hundreds of kilowatts. Agricultural infrastructure is most often funded by bilateral or multilateral donor agencies from industrialised countries. Development of mini-hydropower is presently funded via the Clean Development Mechanism (CDM) defined under the United Nations Framework Convention on Climate Change (UNFCCC). These funding sources are limited so there is a pressing need to optimise the efficiency and impact of investment.

Skilled seasonal forecasts depend upon precise assessment of availability of mass (precipitation) and energy (temperature) inputs to the meltwater-runoff generation system and upon accurate understanding of system responses to variability in these inputs. In the UIB, to be of practical use, forecasts of summer runoff are necessary at the end of winter (late March / early April), thus requiring a lead-time of between 3 and 6 months. For large nival-regime catchments (in the Western Himalaya) where runoff is primarily governed by mass inputs, Archer and Fowler (2008) have shown that skilled forecasts with this length lead-time are possible. For glacial-regime catchments where summer runoff is primarily governed by energy inputs, skilled forecasting remains challenging due to the difficulty of accurately predicting temperature anomalies with an adequate lead-time.

The core understanding of the hydrological behaviour of subcatchments of the UIB needed to enable skilled forecasting is also crucial to providing insight into likely water availability in the next few decades. Further prerequisites for this output are the assessment of the plausibility of available climate projections for the region and then the translation of these projections into likely changes in the mean values and interannual variability of regional hydrological cycles. Relationships identified between the meteorological point observations of temperature and precipitation—two parameters which are also key output

variables in regional climate model (RCM) simulations—and the remotely sensed spatial data products capturing variability at the village/valley catchment scale will guide assessment of the implications of future climate projections on local water availability. These projections will themselves be the result of a rigorous bias assessment and correction methodology applied to the available RCM outputs.

2 Study Area and Data Limitations

2.1 Study Spatial Extents & Limitations of Observed Record

A substantial challenge at present for local water resources management initiatives in the UIB is the availability of hydroclimatological data at the appropriate scales. Sparse, but spatially representative, point observations of temperature and precipitation are available from long record meteorological stations operated by the Pakistan Meteorological Department (PMD). The relatively low station spatial coverage density, however, leaves doubt as to whether this data adequately represents the heterogeneities which may occur at smaller spatial scales. Furthermore, at present, the river gauging data—collected by the Pakistan Water and Power Development Authority (WAPDA)—available to this project is only at the spatial scale of tributary river basins and has little temporal overlap with existing validated spatial climate data products derived from remote sensing imagery. The geographical situation of the primary gauged basins and locations of available local meteorological observations are shown in Fig. 1. A propos, the geographical area referred to as “the NW UIB analysis unit [X]” in later figures is shown in Fig. 1 with hash marks and is comprised of primary gauged catchments ([1] through [4]) plus the Indus main

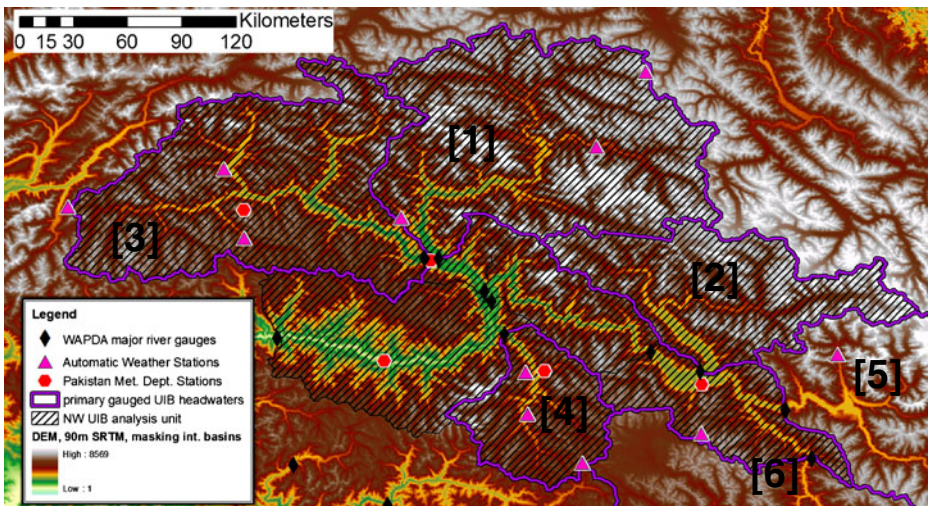


Fig. 1 Primary gauged UIB headwater tributary basins & available local meteorological stations. Primary gauged catchments : [1] Hunza river to Dainyor bridge; [2] Shigar river to Shigar town; [3] Gilgit river to Gilgit town; [4] Astore river to Doyian; [5] Shyok river to Yogo; [6] high Indus to Kharmonj; nb : the NW UIB analysis unit [X] is shown with hash marks and is comprised of [1] through [4] plus Indus main channel gorge from Besham Qila upstream to the gauging stations at Kharmonj and Yugo, the Upper Indus to Besham [0] comprises the NW UIB plus [5] & [6]

channel gorge from Besham Qila upstream to the gauging stations at Kharmong and Yugo. The Upper Indus to Besham [0] comprises the NW UIB plus the primary catchments [5] & [6]. The same number system for the primary gauged catchments is retained in Fig. 2 which shows the geographic location of the village/valley scale case study subcatchments.

The complex geopolitical situation in South Asia, and especially the tensions and suspicions over finite water resources, make data providers hesitant to offer international researchers access to data. We have access to temperature observations up to 31 December 2007 and precipitation observations to 31 August 2010 for primary long record stations. Records of river discharge are deemed more sensitive however and therefore we have only limited access for the period overlapping the MODIS observational record: Astore river 2000–2008; Gilgit river 2000–2008; Hunza river 2001–2004+2008; Indus main channel at Besham Qila 2000–2002. Furthermore, we have access to temperature and precipitation data from more than a dozen automatic weather stations (AWS)—installed at significantly higher elevations than valley-based meteorological stations—for only 1994–1998, which does not overlap with the MODIS record. Even if these issues were resolved, however, they would address only the tributary basin scale and not resolve issues of direct local observations at the scale of the village/valley water resource management.

To overcome these ground-based data limitations, the adequacy of spatial remotely-sensed climate data products to act as analogues for point meteorological observations and the scalability in the climate drivers of hydrological variability between tributary basins and village/valley catchments will be tested. Then the variability of these drivers at the local scale will be directly analysed to characterise the potential hydrological implications for six different spatial aggregations, for each of two different spatial scales. The large scale includes individual (WAPDA) gauged tributary basins and aggregations of the same. The surface area of these spatial units ranges from several thousand to nearly 200,000 km². The second scale is comprised of “case study” examples at the village/valley scale. The cases

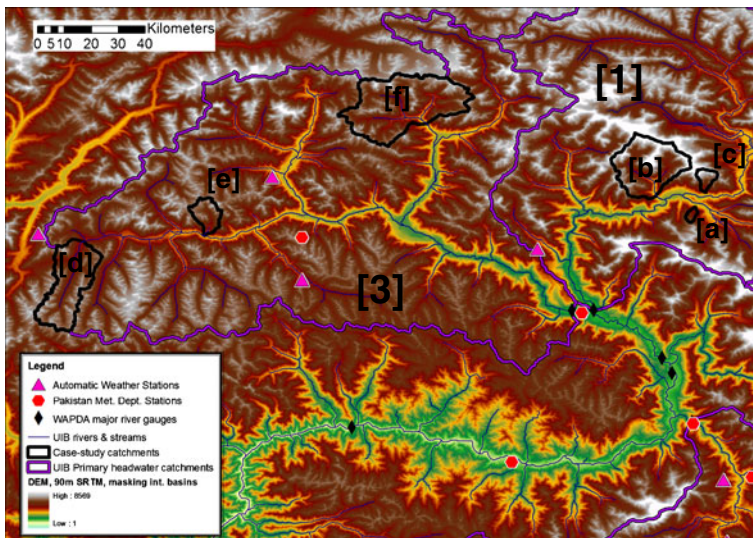


Fig. 2 Detail of example village/valley scale case study catchments. Example case study catchments : **a** Kunjekshal nallah, **b** Hassanabad nallah, **c** Ahmedabad nallah, **d** Langkar meadows, **e** Kasundar nallah & **(f)** Ishkoman valley; for reference, as in previous figure [1] Hunza river to Dainyor bridge and [3] Gilgit river to Gilgit town

were chosen in concert with the NGO's AKRSP and WWF. They represent the catchment areas either : i) from which individual communities abstract a portion of available streamflow to provide water for domestic and irrigation purposes; or ii) distinct ecological zones of interest for conservation and ecosystem services studies. The size of these case study catchments ranges from a dozen km² to a few hundred km².

2.2 Using Remote Sensing for Application in Hydrological Studies

2.2.1 General Limitations of Radiometrically-derived Spatial Climate Data Products

While providing valuable insights into predominant meteorological conditions over vast often sparsely instrumented areas, spatial climate data products do have substantial limitations and shortcomings.

The temporal frequency of remote sensing observations is one important example of these. At present there is an inverse relationship between frequency and (horizontal) spatial resolution. The Moderate Resolution Imaging Spectrometer (MODIS) data products have a maximum horizontal resolution of 500 m to 1 km and are derived from twice-daily overpasses of the target area. The consistent timing and frequency of observation is a result the sun-synchronous (polar) orbits of the “Terra” and “Aqua” Earth Observation System (EOS) satellites on which the MODIS instrument is carried. This spatial resolution provides adequate detail to assess subcatchment-scale conditions, i.e. on the order or tens to hundreds of square kilometres. However, data products with better horizontal resolution (sub 100 m) are necessary for studying smaller spatial areas, such as individual glaciers, and these often have observational frequencies of only once every two weeks or more (e.g. sixteen days for ASTER and Landsat ETM+). In contrast, the remotely-sensed data products with the best frequency of observation—from geostationary satellites—have very coarse spatial resolutions (>250 km), only detailed enough for continental (or synoptic) scale studies.

Radiometrically-derived data products, such as MODIS, also have important limitations in their capacity to accurately assess parameters of interest. The spatial data products have their theoretical basis in identified relationships between the intensity of emission of electromagnetic radiation at specific wavelengths (spectral bands) and specific surface or atmospheric properties. While MODIS data products are quite robust due to the high number of available spectral bands (thirty-six) there is still potential for misidentification of radiometrically similar climate features. This is perhaps best illustrated by the challenge of accurately differentiating snow versus cloud (both are cold and “bright”); crucial as algorithms for determination of snow cover (SCA) and land surface temperature (LST) routinely employ “cloud-masking” approaches. Even the sophisticated MODIS products are sensitive in this regard to a number of thresholds and viewing conditions (Ackerman et al. 2008). In other mountainous study areas, the systematic misidentification of snow as cloud in the transition zone between snow-covered and snow-free areas has been found to occur in earlier versions of the MODIS snow algorithm (Klein and Barnet 2003). The ground-based data available to this study does not allow assessment of whether such issues have been resolved in the current version of the algorithm. Independent of cloud-masking issues, the topography of the study area for mountainous regions may also affect accuracy of snow-cover detection. In winter large shadows resulting from low sun angles can also result in under-detection of snow in steep terrain (Sorman et al. 2007).

Given these limitations, it may be prudent to consider spatial data products as quantitative indicators of hydrometeorological conditions rather than as absolute measures of the physical state of the target catchment.

2.2.2 Remotely-sensed Datasets

This study, in the main, uses snow covered area (SCA) and land surface temperature (LST) data products from the MODIS instrument aboard the NASA Earth Observation Terra platform. The MODIS data presented here were acquired as eight-day temporal aggregates over the period from March 2000 to July 2010. The temporal aggregates cover consecutive Julian days: 01 January to 08 January, 09 January to 16 January, etc. Thus there are forty-six time-steps for each calendar year, with the last aggregate—starting Julian day 361—overlapping the following year by two or three days. For SCA the eight-day rasters provide 500 m horizontal resolution maximum snow cover extent (product MOD10A2) (Hall et al. 2001). For LST the eight-day rasters provide 1 km horizontal resolution mean surface temperature for day-time (near local noon) and night-time (near local midnight) overpasses (product MOD11A2) (Wan 2008). In order to compare the MODIS data to local observations, the eight-day rasters were further aggregated by calculating pixel by pixel means from groups of four eight-day rasters to provide proxies of calendar month averages. This spatio-temporal aggregation is summarised in Table 1.

Assessment of MODIS LST and SCA Validity Using Local Air Temperature Observations In addition to the extensive correlation analyses presented in sections 3 and 4 of this paper, a site-specific direct assessment of the coherence and reasonability of the MODIS data products was conducted for the Astore PMD station and the Astore catchment. While the Astore PMD station measures air temperature at height of 2 m rather than LST, the values for air temperature at the Astore station and LST in the surrounding MODIS pixels would be expected to track closely throughout the common observation period. In order to avoid issues of precision in geolocation, the LST values for direct comparison were extracted from the pixel of the MOD11C3 data product (5 km resolution) covering the Astore PMD station. Average LST was taken as the mean of LST values from daytime (approximately local solar noon) and nighttime (approximately local midnight) satellite overpasses. Average air temperature was taken as the mean of monthly means for daily minimum temperature (Tmin) and maximum temperature (Tmax). LST and air temperature values were compared both as an eight-year (2000–2007) time series and as mean values for each month of the year.

In order to assess the SCA data product an approach used by Jain et al. (2008) for assessment of snow cover mapping for the Satluj (Sutlej) basin was applied here. This method uses the simplified assumption that for mountainous semi-humid catchments SCA will be equal to the fraction of the catchment where mean daily temperature is below freezing (0°C). To determine the latter value, the monthly value for Tavg was applied to the

Table 1 Spatial and temporal resolution

MODIS parameter	snow covered area (SCA)	land surface temperature (LST)
MODIS dataset designation	MOD10A2	MOD11A2
MODIS source spatial resolution	500 m nominal	one kilometre nominal
MODIS source temporal resolution	eight-day maximum	eight-day mean
analogous to local observation parameter	precipitation (cumulative cold season)	two-metre air temperature
further temporal aggregation	means of four eight-day rasters centred on calendar months	means of four eight-day rasters centred on calendar months

hypso-metric information for the catchment—derived from the NASA SRTM 90 m digital elevation model—via a linear lapse rate of 7°C per 1000 m. When the elevation of 0°C isotherm had been calculated, the nominal locally-observed SCA was taken to be equal to 100% minus the cumulative fraction of the catchment below isotherm elevation. These nominal values SCA were compared to the spatial average MODIS SCA values for the Astore catchment both as an eight-year (2000–2007) time series and as mean values for each month of the year.

The results of the comparisons of LST to air temperature and nominal SCA to MODIS SCA are shown in Fig. 3. As can be seen in the upper left panel, LST and air temperature do in fact track very well together as a time series. Of particular note is the agreement in interannual variability of summertime annual maxima. Wintertime annual minima do diverge but this can be understood through annual cycle (Fig. 3, lower left panel) of LST and air temperature. During the winter snow cover is nearly complete and the snow pack surface temperature becomes appreciably colder than the overlying air temperature through the accumulation of thermal inertia, also known as “cold content” (Bras 1990). During the spring and summer as the snow pack warms then melts, and SCA diminishes, the LST and

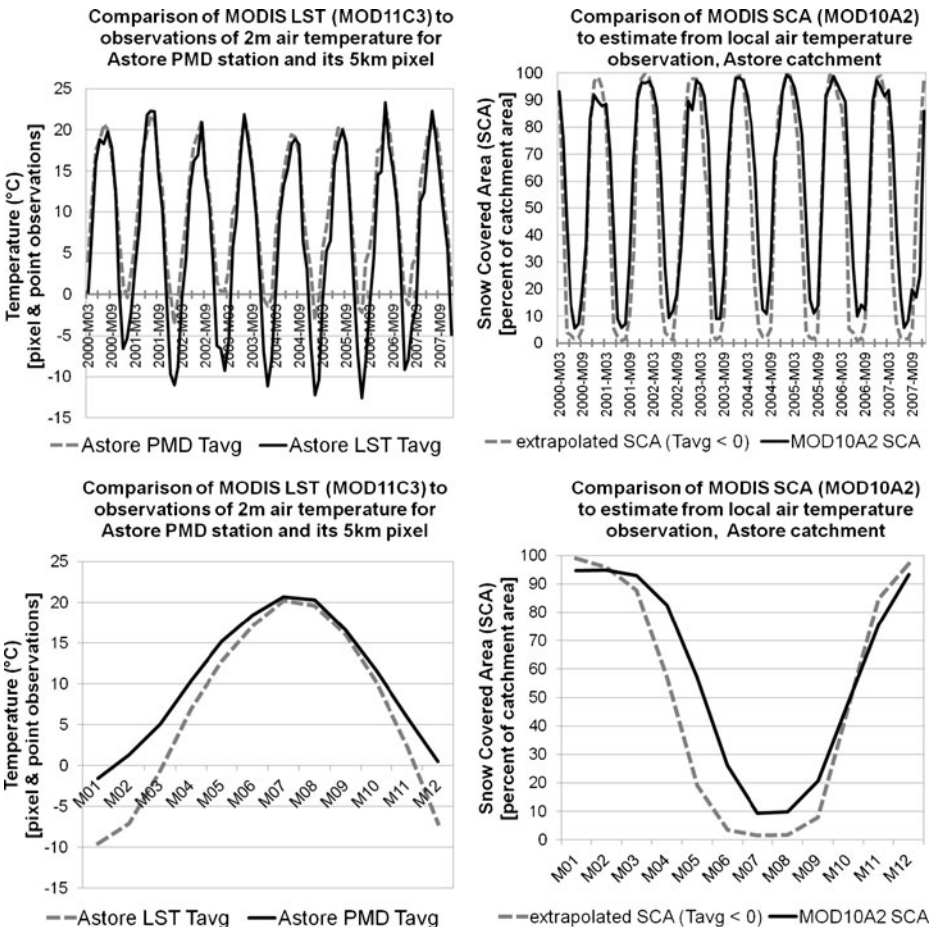


Fig. 3 Assessment of MODIS LST and SCA validity using local air temperature observations

air temperature converge. They then diverge again in autumn and winter as the snow pack accumulates and SCA and snowpack cold content increase.

The plots comparing nominal SCA to MODIS SCA as a time series (Fig. 3 upper right panel) and annual cycle (lower right panel) also demonstrate this relationship. From the time series comparison, interannual variability in the timing and magnitude of annual maximum SCA agree well between the nominal and MODIS values. The divergence appears during the ablation phase while the reduction in SCA (from snow melt) lags the air temperature. Also the simplified nominal SCA from air temperature method does not take into account the presence of a small glaciated area in the Astore catchment, hence underestimation of annual SCA minima. The nominal and MODIS SCA values do, however, converge once again during the accumulation phase (Autumn and Winter).

Assessment of the TRMM 3b43 Data Product A preliminary assessment was also made of the usefulness of the Tropical Rainfall Monitoring Mission (TRMM) precipitation estimates for the region; further detailed analysis is given in Forsythe et al. (in prep.). These are derived from a multi-sensor system which assimilates observations from multiple satellites gauge-adjusted with the Global Precipitation Climatology Project (GPCP) dataset (Huffman and Bolvin 2011). This constellation of data sources includes the TRMM instrument itself which carries a passive microwave imager and space-borne rainfall radar which provide high resolution assessment of precipitation rates within the satellite's window of view (swath width). These high resolution observations are very limited in observational frequency with direct repeat observations only approximately twice per month. The TRMM specific observations, however, are merged with additional passive microwave observations from several other satellite-borne instruments (SSM/I, DMSP, AMSR-E, AMSU-B, etc) as well as the near continuous low-resolution infrared and thermal imagery from geostationary weather satellites. This multi-sensor composite can thus provide a balance between good spatial resolution and high frequency observation, although due to the present limited number of passive microwave-equipped satellites there are substantial gaps in the spatiotemporal coverage of the higher resolution data needed to calibrate the lower resolution continuous imagery from the geostationary platforms (Huffman et al. 2007).

The data are from the 3B43v006 data product which provides a continuous time series of monthly estimated precipitation totals at 0.25 decimal degree horizontal resolution from Jan 1998 to present. Comparisons to available local long-record observations of precipitation and limited river discharge data strongly suggests that the TRMM estimates provide a quantitative indicator of monthly rainfall abundance rather than a measure of absolute magnitude. In this they are similar to the local long-record meteorological observations which also do not directly represent catchment wide precipitation but do correlate well as indicators of mass inputs for seasonal snowmelt driven catchments (Archer 2003; Archer and Fowler 2008).

Specific indications that TRMM does not provide an absolute measure of precipitation over the UIB include:

- [a]. for the very limited time series of overlapping available gauge records of seasonal snowmelt-driven (nival regime) catchments, the TRMM catchment-average accumulated precipitation for each hydrological year is only a fraction (~ 40 to 60%) of the observed river discharge (when converted to runoff depths).
- [b]. the monthwise-contributions to annual total precipitation show substantial disagreement in the seasonality of precipitation distribution between TRMM and both long

record valley observations and AWS located at higher elevations (see Fig. 4). Local observations show a stronger mode of precipitation in spring (March–April–May) with more limited contributions in summer (June–July–August) in comparison with TRMM. This issue of inhomogeneity between TRMM and local observations is further evidenced when comparing scatter plots of TRMM estimates versus local observations filtered by season. As Fig. 5 shows, the ratio of TRMM to local observations is clearly greater in summer than in spring. This may be due to the underestimation of stratiform precipitation—enhanced in the UIB by orographic lifting—compared with the convective precipitation that traditionally dominates in the tropics and sub-tropics where the TRMM initiative is focused. Orographic precipitation poses technical problems for both infrared-derived and passive microwave-based rainfall estimation algorithms (Dinku et al. 2008).

[c]. the TRMM data do not exhibit the marked orographic gradient (increasing precipitation with increasing elevation) that is shown by comparing precipitation totals recorded in PMD valley stations to those measured by the higher-elevation AWS units, when comparing pixels overlying areas of different mean elevation. This again may be due to the underestimation of orographically-driven stratiform precipitation.

More practically, the focus in this study is on identifying opportunities to use spatial data products for assessing conditions within specific contributing areas drawn upon by villages and ecological areas for their water resources. As such, the limited spatial resolution—0.25 decimal degrees, roughly 28 km—of TRMM is not best suited for this purpose. In this context, the role of TRMM data is best considered as equivalent to the observations from (distant) long-record meteorological stations in the primary regional towns, i.e. a strong quantitative indicator but not providing village/valley-scale specificity. For the case studies used here, a minimum horizontal resolution would be 5 km with much better definition resulting from a shift to 1 km resolution. This is precisely the scale of the available MODIS data products. Therefore the analysis will focus on these products.

3 Characterisation of UIB Hydrological Regimes

3.1 Characterisation of Nival and Glacial Regimes from Local Observations

Runoff in the UIB is primarily composed of meltwater from ephemeral snow and perennial glacial masses with a smaller contribution from direct winter or monsoon rainfall from

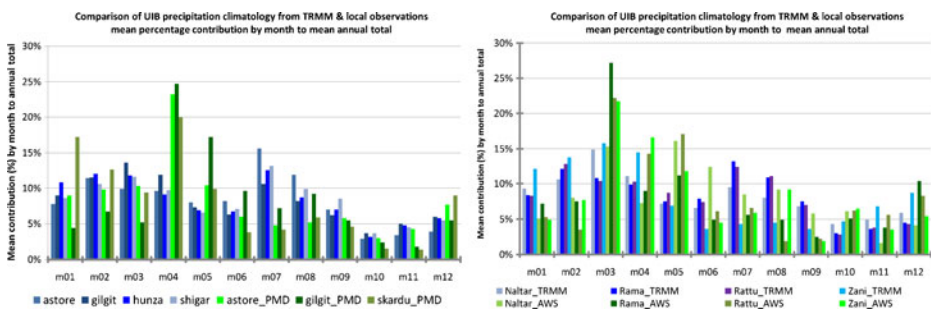


Fig. 4 Comparison of UIB precipitation climatology from local observations & TRMM

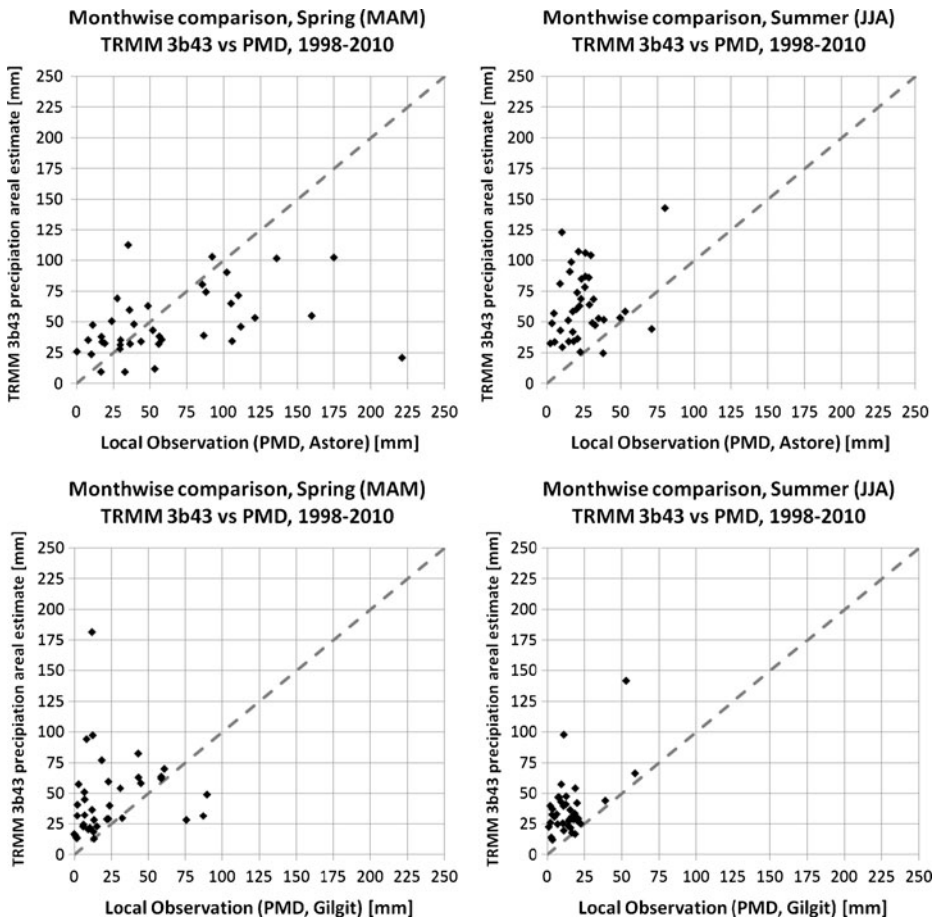


Fig. 5 Monthwise comparison, filtered by season, of local precipitation measures and TRMM estimates

foothill catchments (Archer 2003). The relative contributions from these three sources of runoff (direct rainfall, seasonal snow and perennial ice) define three observed hydrological regimes characterising the sub-catchments within the UIB (Archer 2003). For the case study areas where seasonal snowfall (nival) and glacial regimes dominate, the timing of annual hydrological cycles are shaped by the accumulation of snow and ice from October through March followed by melting of ephemeral snowpack from April through June, with significant ablation of glacial ice in July and August. These cycles are thus driven by the predominant temperature conditions, which can be characterised as the fraction of the catchment where night-time temperatures remain above 0°C. Examples of the annual cycles for nival, glacial and mixed nival-glacial regimes are shown in Fig. 6. In nival regimes, the accession limb of the melt hydrograph rises quickly in spring with warming temperatures but recedes in mid-summer once the seasonal snowpack is exhausted. In glacial regimes the accession limb of the hydrograph lags rising temperatures marginally, but flows remain high until the catchment begins to cool in late summer.

Previous studies (Archer 2003, Archer and Fowler 2008) show significant linear correlations between gauged river flows and observed climate variables, notably concurrent temperature or preceding season precipitation. These relationships differ between the three

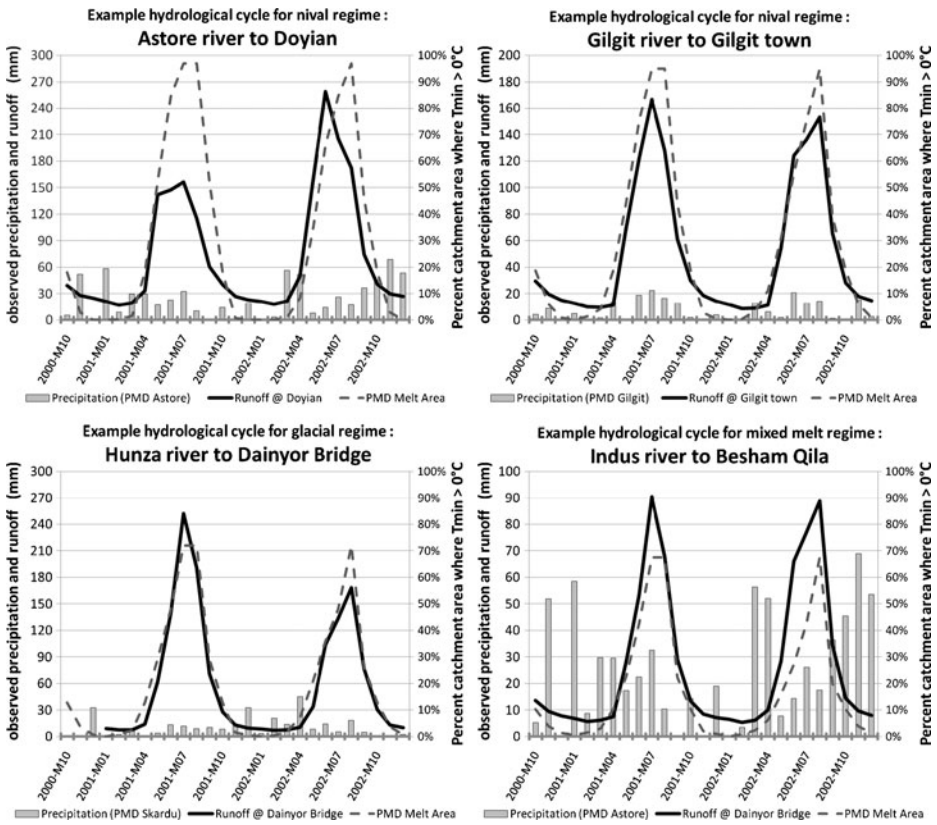


Fig. 6 Annual cycles for UIB hydrological characterised by local observations

identified regimes. Examples of such relationships are shown in Fig. 7 for the Astora catchment, where runoff is primarily snow-melt from winter accumulated snowfall, and for

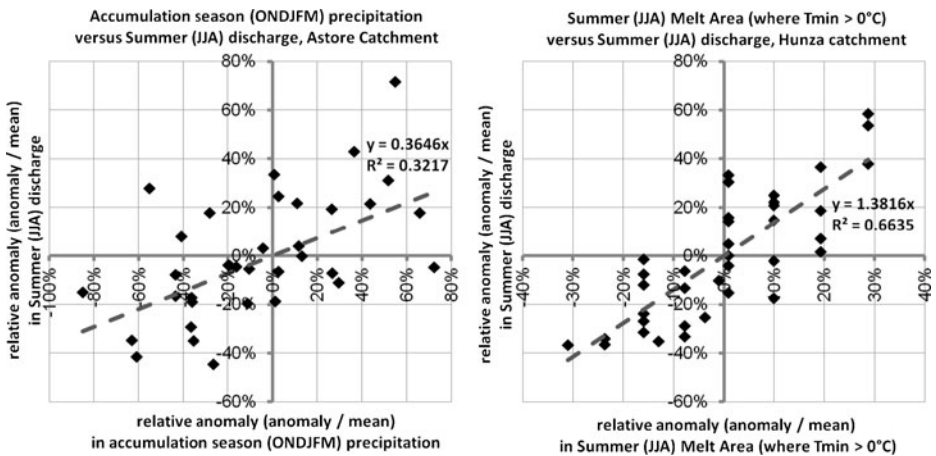


Fig. 7 Example linear relationships between runoff and locally observed climate variables for nival and glacial hydrological regimes

the high level Hunza catchment, which is primarily glacier fed. The indicators, as well as summer (June to August) discharge observations, have been transformed to relative anomalies, i.e. the anomaly is calculated by subtracting the record mean from the individual observation then the result is divided by the record mean. For the nival catchment, Astore, the best indicator is the accumulation season (October to March) precipitation at Astore. For the glacial catchment, Hunza, the best indicator is the fraction of the catchment where the minimum night-time temperature is greater than 0°C as derived from concurrent temperature at Gilgit and linear temperature lapse rates based on available regional observations. Such relationships indicate the sensitivity of UIB hydrology to both climate variability and gradually developing trends.

In the headwater reaches the glacial (perennial ice) and nival (seasonal snowfall) regimes are dominant. In these areas river flows during the melt season, locally referred to as the Kharif—from April to September—dominate annual runoff volumes, with summer (June to August) runoff often accounting for 65 to 75 % of annual totals [Table 2]. Referring again to Fig. 7, the large range of observed interannual variability—+75 to -45% of period mean for a nival regime, +60% to -40% of period mean for a glacial regime—in summer runoff volumes is striking. The coefficients of variation—the ratio of standard deviation to mean—for summer runoff given in Table 2 for the primary gauged catchments range from 13 to 26%. Notably smaller spatial units and areas with one dominant control tend toward the higher end of this scale. This may imply that the village/valley scale sub-catchments of interest in the present work may experience even greater variability due to localised anomalies in mass (precipitation) or energy (temperature) inputs.

3.2 Substitution of Spatial Data Products for Local Observations in the Characterisation of UIB Hydrological Regimes

Thorough examination of the MODIS SCA and LST data products can identify analogues for the ground-based observations used to characterise the hydrological regimes of the UIB.

Table 2 Hydrological characteristics of the large-scale UIB basins

Catchment // River Gauge units	Area (km ²)	Mean Elevation (m)	Annual Total runoff (mm)	Summer (JJA) runoff (mm)	Ratio Summer/ Annual total for runoff fraction	Std. Dev. Summer runoff (mm)	Summer runoff coeff. of variation fraction
Shyok river to Yogo	65,025	4900	160.0	117.0	0.731	30.1	0.257
Indus river to Kachura	146,100	4789	222.7	152.1	0.682	28.8	0.189
Hunza river to Dainyor Bridge	13,925	4472	695.3	501.1	0.720	130.6	0.260
Gilgit river to Alam Bridge	27,525	4094	681.1	475.7	0.698	63.7	0.133
Astore river to Doyian	3,750	3921	1122.9	729.7	0.649	182.8	0.250
Indus river to Besham	196,425	4505	375.9	252.3	0.671	37.5	0.148

A spatial analogue for the “point observation & lapse rate”-derived catchment melt area parameter is a case of straight-forward substitution (direct assessment).

Selection of the best analogue for accumulated cold season (October to March) precipitation from the information contained in the SCA data product, however, is more complex. An initial indication is given by the temporal aspect: the need to characterise the state of the catchment at the transition from accumulation to ablation, i.e. in late March or early April. Thus, one option is to select as an indicator the total catchment SCA in March. This is logical in that the SCA will vary relatively consistently as a function of the seasonal snowline (elevation of the transition between snow-covered and snow-free portions of the catchment). Given the orographically-driven nature of precipitation in mountainous areas, a vertical profile of the accumulated snowpack can be visualised as a wedge beginning at the seasonal snowline and increasing in depth upward toward the elevation of maximum precipitation. This concept is illustrated in Fig. 8 as is the mean variation of SCA versus elevation by month for the late winter and early spring.

Another option for indicator selection is to focus on SCA within an elevation band exhibiting the maximum interannual variability for the season of interest. Figure 9 shows the interannual variability of SCA versus elevation for two nival regime catchments, Astore and Gilgit. The zone of greatest variability, where the information potential of the MODIS data product can be maximised, for the end of the accumulation season lies between 2500 and 3000 m asl. For the purposes of illustration, the SCA within the 2700 m asl elevation band has been used here as an analogue for accumulation season (October to March) precipitation. Figure 10 shows for the two nival regime catchments, Astore and Gilgit, how the 2700 m asl SCA tracks not only with total catchment SCA but also with observed runoff and a crude approximation for snow water equivalent (SWE) extrapolated from TRMM. Figure 11 then presents examples of the annual hydrological cycle for nival, glacial and mixed nival/glacial regimes using spatial data from MODIS. Figure 11 is thus the remote sensing equivalent of local observation-based Fig. 6. For both the figures derived from local observations and from remote sensing we expect variations in the thermal parameter—melt area—to affect timing of flows in all regimes as well as the magnitude of runoff in catchments with strong glacial contributions. For nival regime catchments, we expect the snowpack indicator—accumulation season precipitation and 2700 m SCA respectively for the two data types—to vary with runoff volume during the following melt season. This is perhaps best illustrated by the Astore panel of Fig. 11.

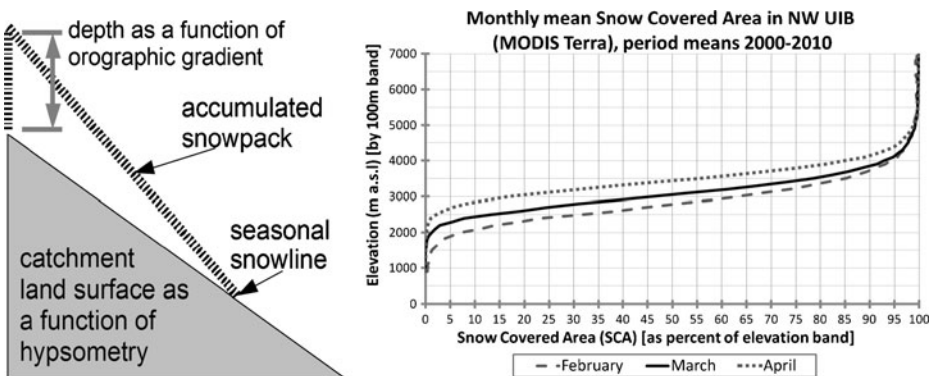


Fig. 8 Conceptual diagram of vertical profile of snowpack depth; SCA versus elevation in seasonal transition from accumulation to ablation

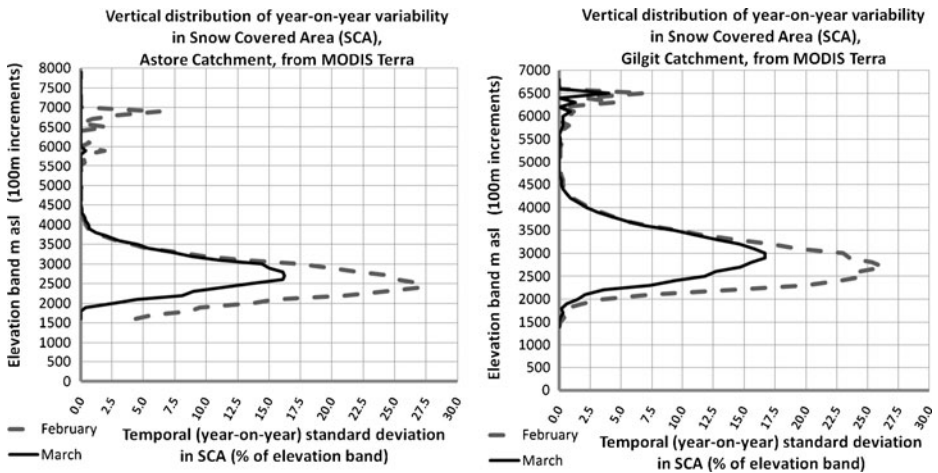


Fig. 9 Vertical distribution of interannual variability in February and March SCA for two nival regime catchments

Examining quantitative linear relationships between the driving climatological parameters (mass input) and hydrological outputs (runoff), Figure 12 shows available indicators of runoff anomalies from local observations, TRMM and MODIS for the nival regime catchments Astore and Gilgit. The same mathematical procedure to calculate relative anomalies used to generate Fig. 7 was applied in Fig. 12. While the very limited available observations—nine each for Astore and Gilgit—are inadequate to assess statistical robustness and quantitative uncertainty, the performance of the available indicators is nevertheless encouraging. TRMM performs well for both catchments, but its spatial scale is too coarse to provide the village/valley scale specificity being sought in the present work. The MODIS March SCA in the 2700 m elevation band also performs moderately well for both catchments, thus supporting its use as an indicator. The performance of the local (point-based) observations is polarised between the two catchments with R^2 values of 0.07 and 0.84 respectively for Astore and Gilgit. This starkly illustrates the pitfalls of conferring excessive significance to samples based on too few observations. Comparison of the panels for Astore in Figs. 7 and 12 show how misleading a randomly chosen subset of observations from the larger record could be in evaluating indicator performance.

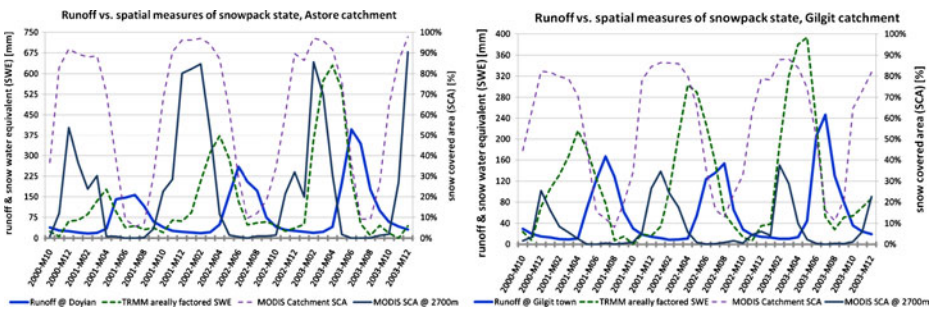


Fig. 10 Time series of runoff in nival catchments and spatial measures of snowpack state

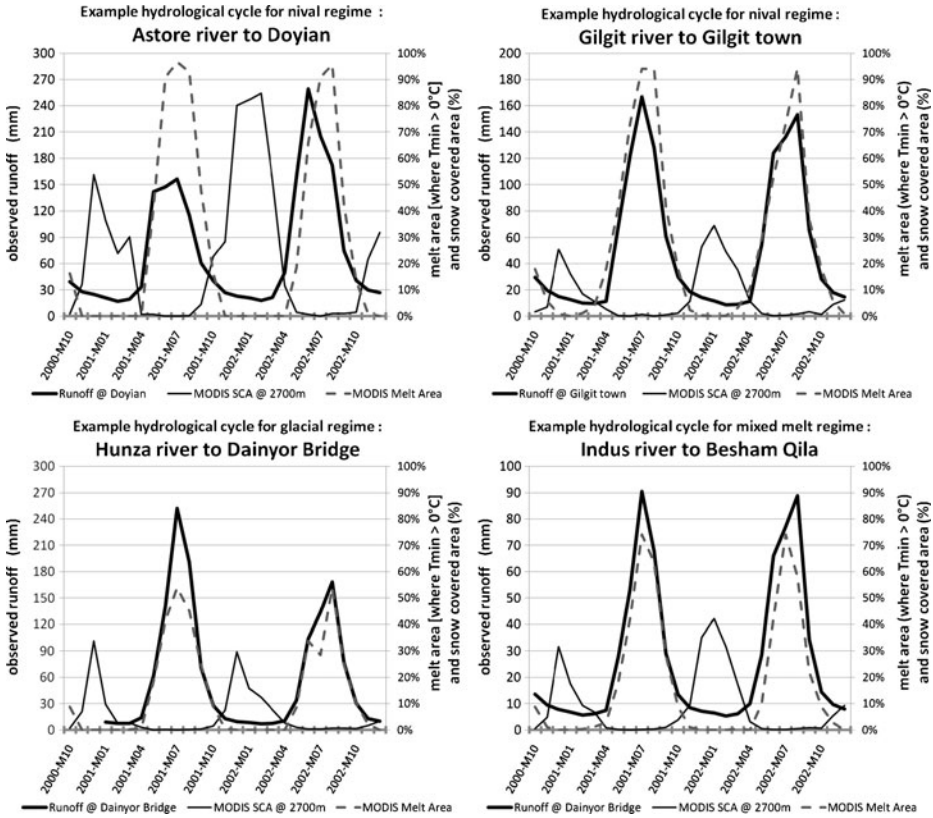


Fig. 11 Annual cycles for UIB hydrological characterised by spatial data

4 Methodology for Validation of Spatial Data Products at the Village/Valley Scale

4.1 Analysis of Relationships Between Spatial Data and Point Observations

The linear relationships between meteorological observations and river discharge previously found by Archer and Fowler (2008) were based on point observations from long record meteorological stations located in permanent settlements (towns) across the UIB. These relatively sparse observations were found to be meaningful predictors of runoff from a vast area. The present work seeks to extend this methodology to use spatial observations from satellite-derived remote sensing data products in order to provide complimentary indicators of mass and energy inputs at finer spatial resolutions than the primary gauged basins. If successful this should enable provision of quantified measures of runoff drivers at a practical scale for local water resources management.

Validity of MODIS SCA as a precipitation analogue was tested by assessing the correlation of normalised, standardised anomalies¹ of March SCA to accumulated cold season (October to March) precipitation. March SCA is roughly the annual maxima of SCA in most sub-catchments. The cold season accumulated precipitation forms the available

¹ Timeseries converted to “normalised anomalies” by subtracting the period mean, then “standardised” by dividing by the period standard deviation.

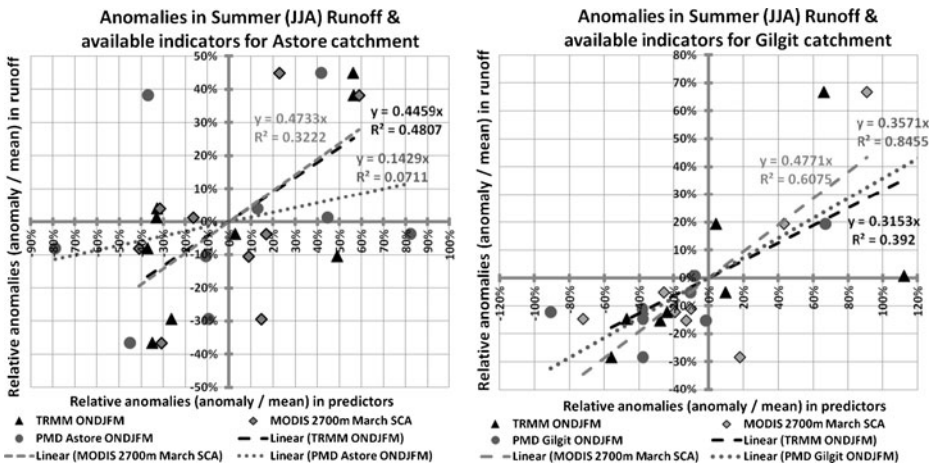


Fig. 12 Example linear relationships between runoff and candidate predictors for two nival regime catchments

snowpack in the UIB before the melt season flood begins. At present this study has local precipitation observations dating from approximately 1960 to the end of 2007. SCA aggregated—i.e. spatial mean—at a range of spatial scales for the series of eight years from 2000 to 2007 was tested against observed precipitation and number of wet days from each of three long-record meteorological stations. The resulting correlations (Pearson’s “r”, 2-tailed significance) are given in Table 3. Although statistical significance is difficult to achieve due to the short duration of the time series, some of the larger catchments as well as the aggregation of the wetter northwestern sector (i.e., excluding Ladakh & Tibet) of the UIB, do show p-values less than 0.05. At smaller spatial scales, including one case study catchment of 10 km², Pearson’s “r” values are regularly greater than 0.5 and often 0.6 for

Table 3 Correlations of March Snow Covered Area (SCA) vs Cumulative Winter (Oct-Mar) Precipitation

Station	Precipitation at Gilgit	Precipitation at Astore	Precipitation at Skardu	Wetdays at Gilgit	Wetdays at Astore	Wetdays at Skardu
Indus to Besham	.358	.590	.086	.466	.455	.307
NW UIB	<u>.800</u>	<u>.760</u>	<u>.647</u>	<u>.825</u>	<u>.678</u>	<u>.776</u>
Hunza to Dainyor	<u>.683</u>	<u>.796</u>	<u>.654</u>	<u>.710</u>	<u>.687</u>	<u>.679</u>
Shigar to Shigar	<u>.696</u>	<u>.732</u>	<u>.604</u>	<u>.692</u>	<u>.686</u>	<u>.847</u>
Gilgit to Gilgit	.587	.452	.496	<u>.634</u>	.378	<u>.666</u>
Astore to Doyian	<u>.673</u>	<u>.722</u>	.265	<u>.816</u>	<u>.671</u>	.535
Ahmedabad nallah	-.526	-.229	-.460	-.364	-.058	-.268
Hassanabad nallah	<u>.727</u>	.475	.528	<u>.616</u>	.414	<u>.721</u>
Ishkoman valley	.433	.328	.446	.465	.279	<u>.622</u>
Kasundar nallah	.481	.300	.460	.460	.162	.468
Kunjekshal nallah	.521	<u>.578</u>	.478	<u>.637</u>	.542	<u>.731</u>
Langkar meadows	.311	.385	.351	.389	.312	.578

Formatting of Tables 3, 4 and 5: values for Pearsons “r” (correlation coefficient) are underlined bold italic if the corresponding significance (p) is less than **0.01**, highlighted in simple bold if p is less than **0.05**

one or more of the tested precipitation variables. Based on these results, SCA appears to be a valid spatial analogue, across the range of tested spatial scales, for point observations of precipitation.

The validity of MODIS LST as an analogue for 2-m air temperature was tested by aggregating groups of four consecutive 8-day day- and night-time LST measures to create a quasi-monthly time series for the duration of the MODIS instrument record. These monthly time-steps were spatially aggregated using a range of catchment scales. The areally averaged values were then assessed for correlation with the same three long-record meteorological stations which were used to validate the SCA data product (point observations available through December 2007 for minimum and maximum temperature). Both LST and 2-m air temperature values were converted to normalised, standardised anomalies to avoid false correlation strength based solely on the annual temperature cycle. The resulting correlations (Pearson's "r", 2-tailed significance) are given in Table 4. Substantial statistical significance ($p < 0.01$) is widespread owing to the larger number of time-steps in the record, compared to the precipitation study. Correlations are generally strong for both day-time/Tmax and night-time/Tmin, though somewhat weaker for the latter, across a range of spatial scales, with the exception of the largest aggregations. This widespread correlation strength supports the validity of LST as a spatial analogue for 2-m air temperature.

Of course patterns of anomalies in the two spatial data products—SCA & LST—are not independent, rather they are climatically coupled. To further test the coherence of the spatial data products, correlations of concurrent anomalies between the variables within individual sub-catchments were assessed. This assessment is a substantial simplification of actual system behaviour as it only considers concurrent anomalies and in no way incorporates specific precipitation input or cumulative effects of prolonged/persistent anomalies. Nevertheless, as shown in Table 5, the sub-catchments under study can be considered quite responsive systems. Given that large temperature anomalies at the monthly timescale may often be due to dominant synoptic conditions thus persisting across the diurnal cycle, the strong correlation between day and night-time LST is largely to be expected. The results of notable (negative) correlations between SCA and day or night-time LST, however, show that at the monthly time-step most sub-catchments show a concurrent response in snow cover to temperature anomalies. These findings further support the use of the available

Table 4 Correlations of Land Surface Temperature (LST) vs 2-m air temperature (point observations)

Station	Astore Tmax vs Tday	Gilgit Tmax vs Tday	Skardu Tmax vs Tday	Astore Tmin vs Tnight	Gilgit Tmin vs Tnight	Skardu Tmin vs Tnight
Indus to Besham	<u>.457</u>	<u>.453</u>	<u>.358</u>	<u>.283</u>	.016	.184
NW UIB	<u>.489</u>	<u>.474</u>	<u>.309</u>	<u>.299</u>	-.082	.227
Hunza to Dainyor	<u>.725</u>	<u>.694</u>	<u>.657</u>	<u>.660</u>	<u>.335</u>	<u>.527</u>
Shigar to Shigar	<u>.736</u>	<u>.655</u>	<u>.679</u>	<u>.665</u>	<u>.310</u>	<u>.528</u>
Gilgit to Gilgit	<u>.671</u>	<u>.709</u>	<u>.590</u>	<u>.662</u>	<u>.219</u>	<u>.564</u>
Astore to Doyian	<u>.747</u>	<u>.710</u>	<u>.647</u>	<u>.664</u>	<u>.339</u>	<u>.532</u>
Ahmedabad nallah	<u>.548</u>	<u>.462</u>	<u>.466</u>	<u>.493</u>	.154	<u>.336</u>
Hassanabad nallah	<u>.637</u>	<u>.613</u>	<u>.587</u>	<u>.571</u>	.198	<u>.401</u>
Ishkoman valley	<u>.603</u>	<u>.576</u>	<u>.543</u>	<u>.590</u>	<u>.261</u>	<u>.477</u>
Kasundar nallah	<u>.591</u>	<u>.666</u>	<u>.552</u>	<u>.606</u>	.184	<u>.535</u>
Kunjekshal nallah	<u>.592</u>	<u>.541</u>	<u>.604</u>	<u>.525</u>	.173	<u>.420</u>
Langkar meadows	<u>.520</u>	<u>.563</u>	<u>.437</u>	<u>.556</u>	.194	<u>.510</u>

Table 5 Correlation between spatial variables within individual sub-catchments

Correlation	besham	nwuib	hunza	shigar	gilgit	astore	ahmed- abad	hassan- abad	ishko- man	kasun- dar	kunjek- shal	langkar
Tday to Tnight	<u>.779</u>	<u>.858</u>	<u>.860</u>	<u>.856</u>	<u>.852</u>	<u>.756</u>	<u>.656</u>	<u>.804</u>	<u>.815</u>	<u>.775</u>	<u>.656</u>	<u>.809</u>
Tday to SCA	<u>-.443</u>	<u>-.414</u>	<u>-.561</u>	<u>-.552</u>	<u>-.603</u>	<u>-.648</u>	<u>-.427</u>	<u>-.509</u>	<u>-.548</u>	<u>-.541</u>	<u>-.454</u>	<u>-.524</u>
Tnight to SCA	<u>-.339</u>	<u>-.286</u>	<u>-.477</u>	<u>-.473</u>	<u>-.496</u>	<u>-.560</u>	<u>-.473</u>	<u>-.410</u>	<u>-.393</u>	<u>-.478</u>	<u>-.315</u>	<u>-.487</u>

spatial data products as analogues for the climatic drivers governing runoff generation in the various sub-catchments of the UIB.

4.2 Analysis of Variability of Snow Cover and Land Surface Temperature

A key consideration in improving the resilience of human systems to cope with climatic perturbations is the accurate assessment of the likely variability of conditions which will be experienced (Wilby and Dessai 2010). Giving local communities the tools to manage existing hydroclimatic variability is a first step toward building capacity for adaptation to potential climate change. It is thus imperative to assess likely variability at the local scale.

It has been shown that runoff in the large gauged tributaries of the UIB is quite variable, especially in the critical summer season during which agricultural activities in the headwater and downstream reaches are concentrated. It has further been shown that available satellite-derived spatial data, MODIS SCA and LST, can be considered adequate analogues for these drivers and that the patterns of anomalies in these data products are coherent over a range of spatial scales.

Figures 13 and 14 show respectively the annual SCA cycles for the gauged tributary basins and village/valley sub-catchments. The mean as well as the 10th and 90th percentiles (c10 & c90 respectively) from the available satellite record are given for each month. Those catchments with little surface area in the lower valley zones tend to have quite high and less variable annual maxima. Those catchments with limited or no area above 6000 m asl tend to have low and highly variable annual minima.

When examining closely the annual SCA minima, the relative variability is striking especially for the smaller village/valley sub-catchments with limited permanent icepack. When focusing on annual minima, the ratio between the period mean and the 10th or 90th percentiles of the available record can be a factor of 2 or more. In water resources management terms either extreme could, in fact, indicate stresses on water supplies. Excessive ablation could indicate insufficient preceding winter precipitation or high summer temperatures whereas high residual snowpack could indicate that insufficient energy was available to drive melting or there was excessive winter snowfall. As will be discussed below, thermal constraints to runoff generation during the summer season are a particular concern in light of observed patterns in 2-m air temperature point anomalies measured at long-record observing stations. On a spatial basis, it was shown above that LST and SCA anomalies have notable (negative) correlation. It has been specifically observed within this record that cool summer anomalies coincide with high (residual) summer SCA anomalies. Unfortunately at present, this project has only minimal access to recent river gauging data from tributary basins to corroborate the hydrological impact of these phenomena.

Daily minimum temperatures are a key element hydrologically in the region because night-time refreezing disrupts meltwater processes (Bengtsson 1982). A key metric for assessing

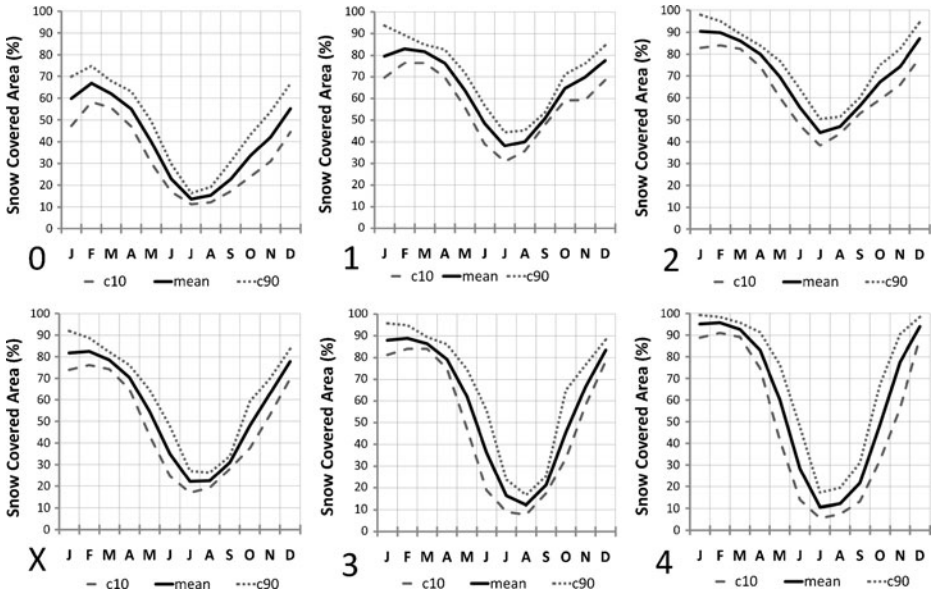


Fig. 13 Annual SCA cycle and interannual variability in major gauged tributary basins from MODIS data. [0] Upper Indus to Besham, [1] Hunza river to Dainyor bridge; [2] Shigar river to Shigar town; [3] Gilgit river to Gilgit town; [4] Astore river to Doyan, [X] NW UIB

thermal constraints to runoff generation is thus the fraction of the catchment in “continuous melt”, i.e. where monthly mean night-time temperatures remain above 0°C. The particular

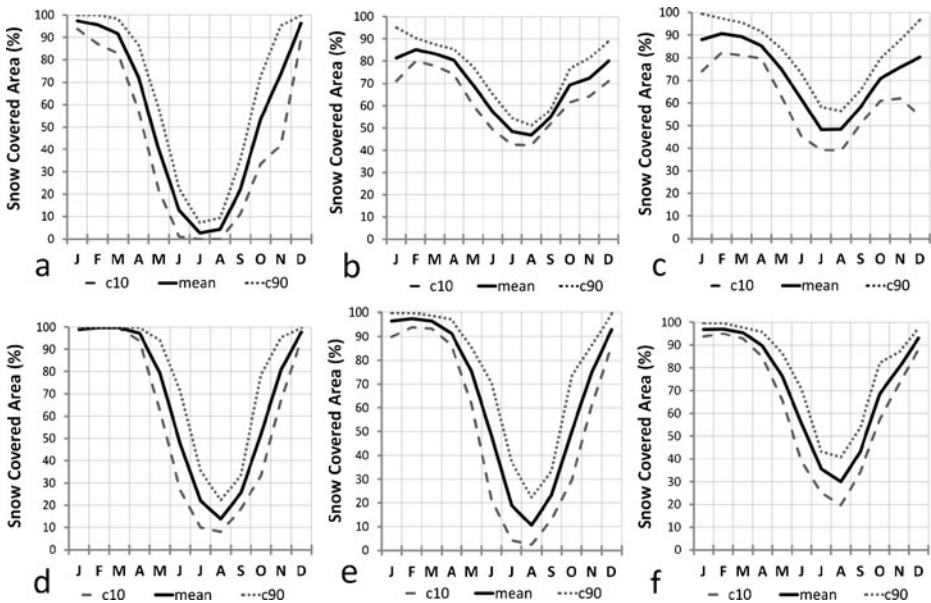


Fig. 14 Annual SCA cycle and interannual variability in example village/valley catchments. **a** Kunjekshal nallah, **b** Hassanabad nallah, **c** Ahmedabad nallah, **d** Langkar meadows, **e** Kasundar nallah & **(f)** Ishkoman valley

hypsometry of the UIB—specifically the concentration of surface area precisely in the elevation range where the 0°C isotherm fluctuates during the summer—means that this parameter is more sensitive to incremental temperature anomalies than one might otherwise expect.

The annual cycle and interannual variability in the continuous melt area are shown for the gauged tributary basins and village/valley sub-catchments in Figs. 15 and 16 respectively. The annual cycle is shown by the “mean” line, while the 10th and 90th percentile lines (c10 & c90 respectively) quantify the interannual variability. These graphical representations of the thermal constraints on ablation processes help us to understand the characteristics of the annual SCA cycle discussed in the preceding paragraphs. The very large degree of variability in June conditions is of particular interest as this is a key month for ablation of ephemeral (seasonal) snowpack. It is also interesting to note the limited relative variability in August conditions, with the exception of some of the very high elevation and widely glaciated catchments. It should further be pointed out that the extremely low values for the month of May in the lower bound line (c10) may be due to apparent night-time low elevation temperature inversions found in this data product (MOD11A2). Additional examination of this facet of LST is being carried out to help determine whether this in fact indicates some physical process or is simply an artefact.

5 Discussion of Implications and Applications of Results

5.1 Implications and Applications of Results for Local Water Resources Management

The considerable interannual variability in both SCA and summer continuous melt area (area with above freezing night-time temperatures) indicates that, in relative terms,

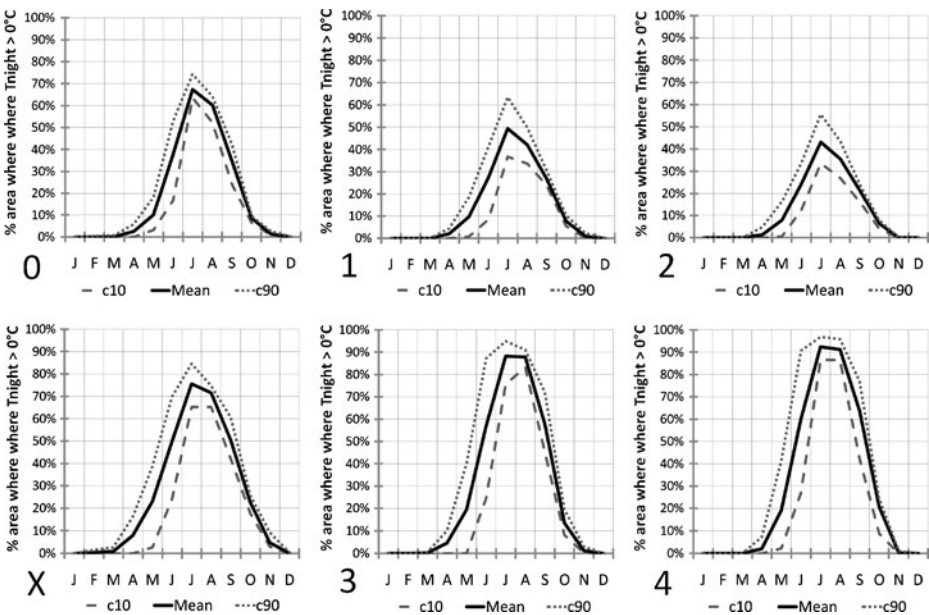


Fig. 15 Annual continuous melt area cycle and interannual variability in major gauged tributary basins. [0] Upper Indus to Besham, [1] Hunza river to Dainyor bridge; [2] Shigar river to Shigar town; [3] Gilgit river to Gilgit town; [4] Astore river to Doyian, [X] NW UIB

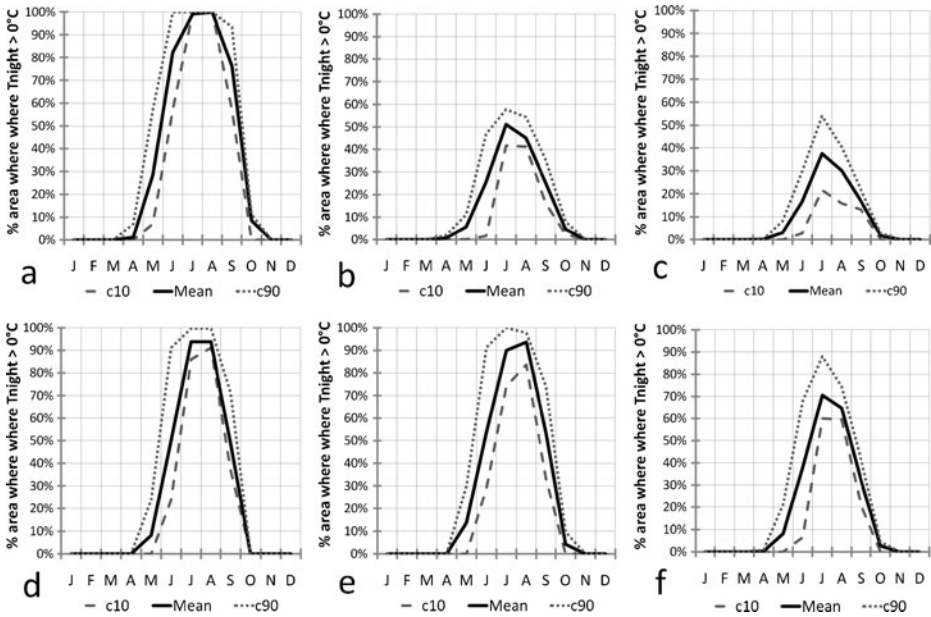


Fig. 16 Annual continuous melt area cycle and interannual variability in example village/valley catchments. **a** Kunjekshal nallah, **b** Hassanabad nallah, **c** Ahmedabad nallah, **d** Langkar meadows, **e** Kasundar nallah & **f** Ishkoman valley

interannual variability in water availability at the village/valley scale is likely to be at least as variable as observed at the gauged tributary basin scale. The high variability of runoff-driving climate parameters in late spring and early summer (May and June) in particular may cause difficulties for small scale irrigation systems during critical phases of crop development. Local development professionals report that in years with low snowpack accumulation some villages experience flows inadequate to meet their needs and emergency measures must be put in place [Sher Khan, AKRSP, personal communication].

Although the presently available observed record is of inadequate length to derive robust quantitative prediction, the potential application of remotely sensed spatial data products as predictors for seasonal forecasting may eventually help to provide early warnings of potential water shortages thus giving local decision makers time to put relief measures in place. If on the other hand, forecasting indicates potentially abundant runoff, local communities may wish to capitalise on favourable conditions by planting the maximum available irrigated area. In either case, because mass inputs in the UIB primarily accumulate throughout the winter/rabi season (October to March)—before the summer melt begins—it is possible to assess them through direct observation and remote sensing with an adequate lead-time for useful forecasting. The effects of varying energy inputs, however, are concurrent to meltwater processes and thus inherently more difficult to quantify as there is a cascade of uncertainty which accumulates through the use of multiple predictors. At the present level of understanding of UIB climatology, skilled prediction of summer temperature with adequate lead-times remains problematic, although it is hoped that on-going research will lead to advances in this domain. This research should specifically focus on predictors which are freely and reliably available with lead times of four to six months. Candidate predictors will include antecedent regional conditions—quantified using remote sensing—and indicators of large scale atmospheric phenomena (teleconnections) which shape global weather variability.

Looking beyond year to year operational management decisions, the climatic changes implied by recent observed trends or projections from RCM simulations may have profound effects on water availability at the village/valley scale in the UIB. Archer and Fowler (2004), Fowler and Archer (2006) have identified significant UIB regional trends toward warmer winters, cooler summers and generally greater precipitation. Summer cooling is of particular concern for local water resources as the observed temperature decreases are driven by falling minimum (night-time) temperatures. As described above, night-time/minimum temperatures are critical in meltwater runoff generation processes. Decreasing UIB summer temperatures, and or water availability in the future, could lead to decreasing yields in marginal (higher elevation) farmland placing further pressure on limited valley-floor irrigated areas. These (relatively) low-lying areas, however, as strikingly illustrated during the extreme summer 2010 monsoon events, are particularly vulnerable to damage from flash-flooding and debris flows. While the probable future frequency of extreme precipitation events in the UIB remains subject to considerable uncertainty, available evidence does not support this risk decreasing under likely scenarios of change (Frich et al. 2002; IPCC 2007). The confident characterisation of future water availability and its variability—upon which improved infrastructure design and long term planning depend—derives from an accurate understanding of responses of the UIB hydro-climatological system to external forcings and confident projections of those forcings in the future. Attainment of this goal would be extremely rewarding in its benefits for regional development, but the task is extremely difficult. Ongoing research in parallel to that presented here seeks both to identify the relationships between large scale climatological phenomena and hydro-climatological responses as well as to assess the ability of existing regional climate models (RCMs) to accurately capture these responses in control/baseline (1961–1990) simulations.

5.2 Opportunities and Imperatives for Future Development of This Methodology

5.2.1 Complimentary Nature of Ground-based Observations and Remote Sensing

We consider that the approach developed in this work clearly demonstrates the essential complementary nature of the two data sources: ground-based observations and remote sensing. Local, ground-based observations are critical to enable the validation of remotely sensed data products. Remote sensing imagery in turn can demonstrate that variability observed at ground-based point observations is representative of the evolution of catchment-scale climate conditions. Thus, given the synergistic nature of the two sources, the ideal instrumentation trajectory would be to reinforce both rather than see one supplant the other. Without improved access to the existing observational record for the present network of AWS units it is difficult to quantify the potential benefits from an increased spatial density of ground-based measurements. However, given the critical importance of the UIB water resources to Pakistan's food security and power supply, it seems reasonable that the relatively modest sums involved in expansion of the AWS network would pay significant dividends in terms of improved operational planning and infrastructure design.

5.2.2 Desirable Advances in Remote Sensing to Support Local Water Resources Management

While the approach presented in this paper demonstrates that currently available remote sensing data products have considerable potential to support local water resources

management, further improvements in spatial data products would of course enhance this potential. Currently available remote sensing data products impose a trade-off between spatial resolution and frequency of observation. Given the topographic complexity of the UIB, high spatial resolutions are essential and remote sensing imagery coarser than that utilised in this study will have limited specificity at the scale of the case studies presented here. Further improvements in spatial resolution would improve characterisation of vertical gradients in SCA and LST and reduce problems of pixel classification in mixed-state (partial snowcover) conditions.

The frequency of observation is also crucial, not only to adequately capture variability in the climate drivers of the hydrological cycle, but also because the present algorithms for SCA and LST require cloud-free conditions which in the UIB can be rare, especially at high elevations. Thus even with daily observations aggregated in eight-day periods it may not be possible to assess snow cover state or land surface temperature for all pixels in a given scene. Further improvements in the frequency of observation would maximise the chances of cloud-free conditions.

Beyond the MODIS data products that are the focus of this work, improvements in the physical accuracy and spatial resolution of direct estimates of catchment mass inputs—precipitation and snowpack water equivalent (SWE)—would be extremely useful. For precipitation estimates provided by TRMM, improvement of physical accuracy could come through improved measurement of orographically driven stratiform precipitation. The planned successor mission to TRMM, the Global Precipitation Mission (GPM) is designed to improve measurement of light rainfall, and snowfall through improved radiometric capacities (Wang et al. 2009). In terms of direct estimation of accumulated SWE in the seasonal snowpack, radical evolution of available remote sensing products would seem to be necessary in order for these products to become applicable to the UIB and similar environments given that present datasets : i) have relatively coarse spatial resolution of 15 km to 25 km, ii) are impeded over complex topography (Foster et al. 2009), and iii) “saturate” for snowpack thicknesses which are relatively small, less than 100 cm, in comparison with the prevailing UIB conditions (Das and Sarwade 2008).

Another difficulty, and thus opportunity for improvement, with the methodology presented here is the very limited historical record length of the available remote sensing data products. This short record length is inadequate to fully represent the range of likely hydroclimatological variability. A solution to this problem is the creation of customised spatial data products using existing primary radiometric observations from a succession of satellite-borne instruments originally launched to support weather forecasting. For example parallel work to that presented here is currently underway by the authors and their collaborators on the development of multi-decadal spatial data products—equivalent to MODIS SCA and LST—using imagery from the Advanced Very High Resolution Radiometer (AVHRR) instrument flown on several generations of (US) National Oceanic and Atmospheric Agency (NOAA) satellites (Chokmani et al. 2005; Khlopenkov and Trishchenko 2006; Li and Becker 1993; Pinheiro et al. 2006). The AVHRR data has similar spatial resolution and observational frequency to the MODIS data products, though with more limited spectral resolution—only five bands—than the more modern instrument. The AVHRR record does, however, extend with variable availability from 1978 to the present. This long record offers the potential to : i) greatly increase the overlap of the spatial data products with local observations, thus refining quantification of relationships between them; and ii) to extend the range of observations to better capture present spatio-temporal climate variability.

5.2.3 Potential Applicability of This Methodology to Other Mountainous Regions

Given the widespread challenges of water resources management in mountainous regions, the potential applicability of the methodology presented here to similar areas is quite pertinent. The core of this methodology hinges on the rigorous characterisation of the local hydrological regime or regimes and the associated climatological drivers. Determination of the meteorological parameters that govern runoff in the case study area is the prerequisite to identification of adequate spatial data analogues. It is possible that this approach may function better for mountain hydrological regimes, such as those presented here, where the accumulation and ablation seasons are distinct than for regimes where snowpack accumulation and ablation are concurrent, as in areas where a monsoonal precipitation regime coincides with the high elevation warm season. Such determinations, however, are beyond the scope of the present study.

6 Conclusions

Local communities in the headwater reaches of the UIB face considerable challenges to their development from highly variable water resources. These resources, if well managed however, also present considerable opportunity for sustainable development and improvement to local living standards. Improved understanding of local hydrology and the climatological processes which drive it is thus essential to supporting local development.

Previous studies have established that predictive relationships exist between meteorological point observations and discharge in the large gauged tributary basins of the UIB. The work presented above demonstrates that remotely-sensed spatial data products (MODIS SCA and LST) can provide adequate analogues for these point observations and that anomalies scale well across a wide range of catchment sizes (areas). These findings open the door to application of knowledge about large-scale UIB hydrology to the level of villages and valley catchments.

Consideration of the variability observed simply in the record of the available data products (early 2000 to present) alone indicates considerable potential hydrological variability in key seasons for local water resource management. These insights will now be applied in concert with locally active non-governmental organisations (NGOs) to assess the risks to and opportunities for improving existing infrastructure and resource management. In addition, demonstration of the scaling relationships will allow application at the village/valley level of improving understanding of potential future hydro-climatological change. Furthermore, if successful the on-going work using AVHRR data to construct a multi-decadal spatial record of SCA and LST would both allow direct estimation of recent trends and assessment of relationships between these regional patterns and larger scale atmospheric phenomena.

In conclusion, helping NGOs & local communities to quantitatively understand the present degree of interannual hydrological variability as well the direction of potential change and the resulting vulnerabilities should help them to better prepare, adapt and plan for current and future conditions. The spatial data products assessed here will form a key component of analysis tools needed to provide this support.

Acknowledgements Nathan Forsythe was supported by a Graduate Research Fellowship award from the US National Science Foundation as well as by project-based support from the British Council and the School of Civil Engineering & Geosciences of Newcastle University. Hayley Fowler was supported by NERC Postdoctoral Fellowship award NE/D009588/1 (2006–2010). Funds for travel between the UK and Pakistan

and for capacity building activities were provided by the British Council through its PMI2Connect and INSPIRE research exchange award programmes. We wish to thank the Pakistan Meteorological Department and the Water and Power Development Authority for the provision of climate and flow data.

References

- Ackerman SA, Holz RE, Frey R, Eloranta EW, Maddux BC, McGill M (2008) Cloud detection with MODIS. Part II: Validation. *J Atmos Ocean Tech* 25:1073–1086. doi:10.1175/2007JTECHA1053.1
- Archer DR (2003) Contrasting hydrological regimes in the upper Indus Basin. *J Hydrol* 274(1–4):198–210
- Archer DR, Fowler H (2004) Spatial and temporal variations in precipitation in the Upper Indus Basin, global teleconnections and hydrological implications. *Hydrol Earth Syst Sci* 8(1):47–61
- Archer DR, Fowler HJ (2008) Using meteorological data to forecast seasonal runoff on the River Jhelum, Pakistan. *J Hydrol* 361(1–2):10–23
- Archer DR, Forsythe N, Fowler HJ, Shah SM (2010) Sustainability of water resources management in the Indus Basin under changing climatic and socio economic conditions. *Hydrol Earth Syst Sci* 14:1669–1680. doi:10.5194/hess-14-1669-2010
- Bengtsson L (1982) The importance of refreezing on the Diurnal Snowmelt Cycle with application to a Northern Swedish catchment. *Nord Hydrol* 13:1–12
- Bras RL (1990) Snowpack and snowmelt. In: *Hydrology: an introduction to hydrologic science*. Addison-Wesley Publishing Company pp. 247–281.
- Chokmani K, Bernier M, Slivitzky M (2005) Suivi spatio-temporel du couvert nival du Québec à l'aide des données NOAA-AVHRR. *Revue des sciences de l'eau / Journal of Water Science*, 19(3):163–179. <http://id.erudit.org/iderudit/013536ar>.
- Das I, Sarwade RN (2008) Snow depth estimation over north-western Indian Himalaya using AMSR-E. *Int J Rem Sens* 29(14):4237–4248. doi:10.1080/01431160701874595
- Dinku T, Chidzambwa S, Ceccato P, Connor SJ, Ropelewski CF (2008) Validation of high-resolution satellite rainfall products over complex terrain. *Int J Rem Sens* 29(14):4097–4110. doi:10.1080/01431160701772526
- Fowler HJ, Archer DR (2006) Conflicting signals of climatic change in the upper Indus Basin. *J Climate* 19(17):4276–4293
- Foster JL, Hall DK, Kelly REJ, Chiu L (2009) Seasonal snow extent and snow mass in South America using SMMR and SSM/I passive microwave data (1979–2006). *Remote Sens Environ* 113(2):291–305. doi:10.1016/j.rse.2008.09.010
- Frich P, Alexander LV, Della-Marta P, Gleason B, Haylock M, Klein Tank AMG, Peterson T (2002) Observed coherent changes in climatic extremes during the second half of the twentieth century. *Clim Res* 19:193–212
- Hall DK, Riggs GA, Salomonson VV, Barton JS, Casey K, Chien JYL, DiGirolamo NE, Klein AG, Powell HW, Tait AB (2001) Algorithm Theoretical Basis Document (ATBD) for the MODIS Snow and Sea Ice-mapping Algorithms. <http://modis-snow-ice.gsfc.nasa.gov/atbd01.html>.
- Huffman GJ, Bolvin DT (2011) TRMM and other data precipitation data set documentation. Laboratory for Atmospheres, NASA Goddard Space Flight Center and Science Systems and Applications, Inc. ftp://precip.gsfc.nasa.gov/pub/trmmdocs/3B42_3B43_doc.pdf.
- Huffman GJ, Adler RF, Bolvin DT, Gu G, Nelkin EJ, Bowman KP, Hong Y, Stocker EF, Wolff DB (2007) The TRMM Multisatellite Precipitation Analysis (TMPA): quasi-global, multiyear, combined-sensor precipitation estimates at fine scales. *Journal of Hydrometeorology* 8(1):38–55. doi:10.1175/JHM560.1
- IPCC: Climate Change (2007) The Physical Science Basis, Contribution of Working Group I to the Fourth Assessment Report of the Intergovernmental Panel on Climate Change. In: Solomon S, Qin D, Manning M, Chen Z, Marquis M, Averyt KB, Tignor M, Miller HL (eds) Cambridge University Press, Cambridge, UK and New York, NY, USA.
- Jain SK, Goswami A, Saraf AK (2008) Accuracy assessment of MODIS, NOAA and IRS data in snow cover mapping under Himalayan conditions. *Int J Rem Sens* 29(20):5863–5878. doi:10.1080/01431160801908129
- Khlopenkov KV, Trishchenko AP (2006) SPARC: new cloud, snow, and cloud shadow detection scheme for historical 1-km AVHRR data over Canada. *J Atmos Oceanic Technol* 24(3):322–343. doi:10.1175/jtech1987.1

- Klein AG, Barnet AC (2003) Validation of daily MODIS snow cover maps of the Upper Rio Grande River Basin for the 2000–2001 snow year. *Remote Sens Environ* 86:162–176. doi:[10.1016/S0034-4257\(03\)00097-X](https://doi.org/10.1016/S0034-4257(03)00097-X)
- Li ZL, Becker F (1993) Feasibility of land surface temperature and emissivity determination from AVHRR data. *Remote Sens Environ* 43:67–85
- Pinheiro ACT, Mahoney R, Privette JL, Tucker CJ (2006) Development of a daily long term record of NOAA-14 AVHRR land surface temperature over Africa. *Remote Sens Environ* 103:153–164. doi:[10.1016/j.rse.2006.03.009](https://doi.org/10.1016/j.rse.2006.03.009)
- Sorman AU, Akyurek Z, Sensoy A, Sorman AA, Tekeli AE (2007) Commentary on comparison of MODIS snow cover and albedo products with ground observations over the mountainous terrain of Turkey. *Hydrol Earth Syst Sci* 11:1353–1360
- Wan Z (2008) New refinements and validation of the MODIS land-surface temperature/emissivity products. *Remote Sens Environ* 112:59–74. doi:[10.1016/j.rse.2006.06.026](https://doi.org/10.1016/j.rse.2006.06.026)
- Wang NY, Liu C, Ferraro R, Wolff D, Zipser E, Kummerow C (2009) TRMM 2A12 land precipitation product—status and future plans. *J Meteorol Soc Jpn* 87A:237–253. doi:[10.2151/jmsj.87A.237](https://doi.org/10.2151/jmsj.87A.237)
- Wilby RL, Dessai S (2010) Robust adaptation to climate change. *Weather* 65(7):180–185. doi:[10.1002/wea.543](https://doi.org/10.1002/wea.543)